Electron and Ion Transport in Tantalum Capacitors

under Steady-State Bias Conditions

M. Kuparowitz

Czech Noise Research Laboratory, Brno University of Technology
Technicka 8, 616 00 Brno, Czech Republic mailing address continued
Email: xkupar00@stud.feec.vutbr.cz

INTRODUCTION

Degradation of leakage current (DCL) under steady-state bias conditions was investigated at temperature 400 K and rated voltage 35 V on samples of solid tantalum capacitors with manganese oxide cathode of three world producers. High temperature and high voltage applications of these capacitors are considered to be limited by ions diffusion and field crystallization mechanisms [1 to 6]. Crystalline oxide starts the recrystallization at temperature above 400 K without electric field. In electric field the recrystallization of tantalum pent-oxide can start at temperature as low as 400 K. Tantalum capacitor is here considered as a Metal – Insulator – Semiconductor (MIS) structure.
I-V characteristics in normal and reverse mode were measured for temperatures 300 and 400 K. Further, the variations of leakage current during the thermal annealing were measured with time in the presence and absence of the external electric field, and evaluated. From these experiments information was received concerning the leakage current conduction mechanism. The leakage current values increase after temperature annealing at 400 K at rated voltage for 550 hours for some samples by up to 2 orders of magnitude.
During annealing the drift-diffusion process is affected by concentration gradient of ions near Ta_2O_5–MnO_2 interface. This paper documents the dependence of electron and ion transport parameters of tantalum capacitors on the particular technology used by three different world producers. Experiments were started with measurement of I-V characteristics at temperature 300 K and theirs analysis.

I-V CHARACTERISTICS ANALYSIS

We will give analyses of electron transport in tantalum capacitors with MnO_2 cathode. Three sets of samples, seven samples each, were studied:

1. Set LM 1 of producer A, case V, capacitance 15 μF, rated voltage 35 V.
2. Set LN1 of producer B, case D, capacitance 15 μF, rated voltage 35 V.
3. Set LT8 of producer C, case D, capacitance 33 μF, rated voltage 35 V.

I-V characteristics in normal modes – NM (tantalum anode is positive) and reverse modes – RM (tantalum anode is negative) contain information on Ta_2O_5 insulating layer structure, electron affinity, band structure and potential barriers on cathode and anode interfaces [2, 3, 7].

I-V CHARACTERISTICS IN NORMAL MODE AT TEMPERATURES 300 K AND 400 K

Experimental results measured at temperature T = 300 K for sample LM1-2 are shown in Fig. 1. The dominant current transport mechanism in normal mode is ohmic for electric field less than 1 MV/cm and for higher value of electric field tunneling electron transport is observed [3].

We will obtain the components of DCL from *I-V* characteristic analyses. DCL consists from two parallel current components, which could be described as:

$$I = G_{\Omega}U + G_T U^2 \exp\left(U_T/U\right) \tag{1}$$

Where G_{Ω} = 690 pS is Ohmic conductivity, G_T = 3,5 nS/V and U_T = 214 V are tunneling current parameters.
Experimental results measured at temperature T = 400 K for sample LM1-2 are given in Fig. 2. DCL consists from 3 parallel current components which could be described as:

$$I = G_{\Omega}U + G_{PF}U \exp\left(\beta_{PF}\sqrt{U}\right) + G_T U^2 \exp\left(-U_{T0}/U\right) \tag{2}$$

Where G_{Ω} = 55,9 nS is Ohmic conductivity, G_{PF} = 68 pS, β_{PF} = 1,12 $V^{-0,5}$ are parameters of Poole-Frenkel current component and G_T = 3,5 nS/V, U_T = 214 V are tunneling current parameters.

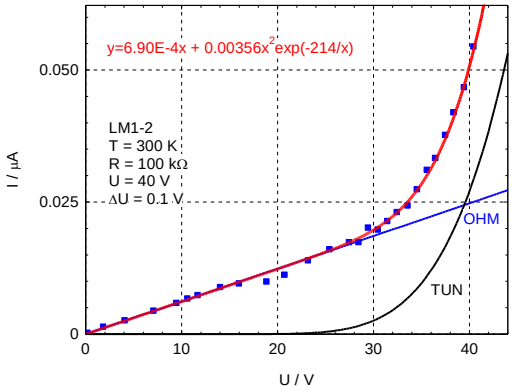

Fig. 1. *I-V* characteristic of sample LM1-2 at temperature 300 K

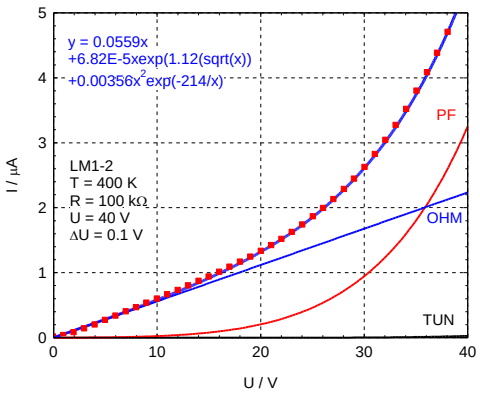

Fig. 2. I-V characteristic of sample LM1-2 at temperature 400 K

Bar chart diagram of DCL at applied voltage U = 35 V and temperature 400 K is shown in Fig. 3 for all the samples of ensemble LM1. Mean value of DCL at rated voltage is I_{av} = 4.76 μA and standard deviation I_{std} = 5.8 μA.

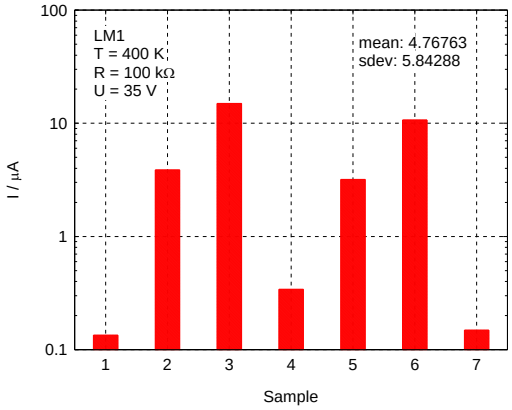

Fig. 3. Bar chart diagram of DCL for U = 35 V and temperature 400 K for all samples of ensemble LM1

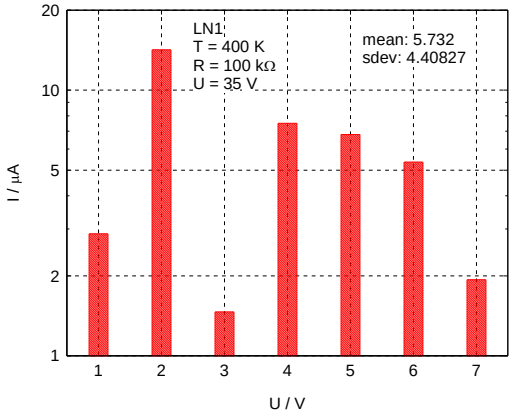

Fig. 4. Bar chart diagram of DCL for U = 35 V and temperature 400 K for all samples of ensemble LN1

Bar chart diagram of DCL at applied voltage U = 35 V and temperature 400 K is shown in Fig. 4 for all the samples of ensemble LN1. Mean value of DCL at rated voltage is I_{av} = 5.7 μA and standard deviation I_{std} = 4.4 μA.

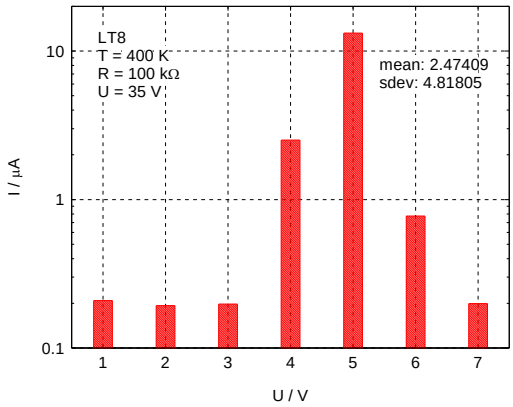

Fig. 5. Bar chart diagram of DCL for U = 35 V and temperature 400 K for all samples of ensemble LT8

Bar chart diagram of DCL at applied voltage U = 35 V and temperature 400 K is shown in Fig. 5 for all the samples of ensemble LM1. Mean value of DCL at rated voltage is I_{av} = 2.47 μA and standard deviation I_{std} = 4.8 μA.

LEAKAGE CURRENT CHANNGES DURING LONG TERM THERMAL ANNEALING

A typical variation of DCL with time of thermal annealing at fixed temperature 400 K and applied voltage U = 35 V in normal mode is shown in Fig. 6. The slope of DCL time dependence can be calculated as the first derivative *dI(t)/dt*.

The leakage current is increasing in time with the decreasing slope. Slope at the beginning of ageing is of the order 100 pA/s, and it decreases exponentially as shown in Fig. 6.

DCL at the beginning of thermal annealing increases with time linearly, which can be expressed as:

$$I_{(t)} = I_0 + mt \tag{3}$$

Where I_0 = 4 μA and m = 146 pA / s for sample LM1-2 at temperature 400 K.

DCL time dependence during thermal annealing in the whole time interval can be fitted by equation:

$$I = I_0 + I_1\left(1 - \exp\left(-\left(t/\tau\right)^n\right)\right) \tag{4}$$

Where I_0 = 4 μA, I_1 = 18.2 μA, τ = 1.39x10^5 s, n = 0.905 for time of ageing 10^5 s. During the long term application of electric field at elevated temperature the drift-diffusion motion of ions (these are probably oxygen vacancies) influences the DCL value. The drift motion of positive ions in electric field leads to the increase of ion concentration in the vicinity of Ta_2O_5 – MnO_2 interface. The diffusion process in Ta_2O_5 starts due to the gradient of ion concentration.
The diffusion process grows prominent with the time of ageing, while the value of the exponent n decreases, as is shown in Fig. 7, where exponent n = 0.846.

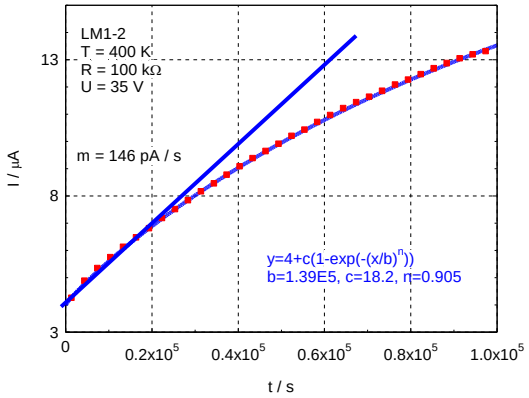

Fig. 6. DCL vs. time characteristic of sample LM1-2 at temperature 400 K

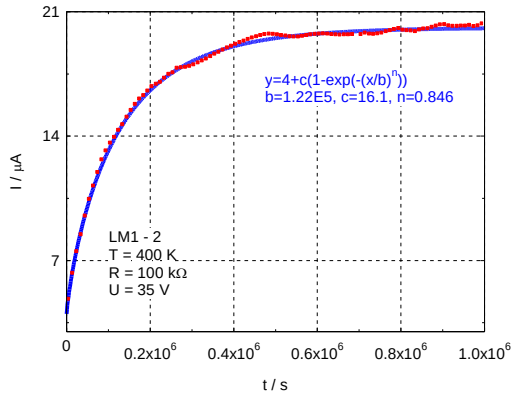

Fig. 7. DCL vs. time characteristic of sample LM1-2 at temperature 400 K

We have found that for all the samples the slope of DCL decreases with ageing time but we have not observed any saturation of DCL value even after 550 hours of thermal treatment. Degradation of DLC during life tests of solid tantalum capacitors has been reported in [3] where the increase in DCL was up to 3 orders of magnitude.

REVERSIBILITY OF DCL CHANGES

When the sample is shorted or lower electric field is applied, a recovery of DCL value is observed. In this case the diffusion process became dominant. Ions accumulated close to the Ta_2O_5 – MnO_2 interface diffuse due to the concentration gradient up to reaching the homogeneous concentration in whole Ta_2O_5 volume. In this case ions are moving from cathode to anode. The drift-diffusion process depends on temperature excitation and it is similar to Brown motion. In our experiment for DCL recovery we applied voltage U = 5 V on the measured samples.

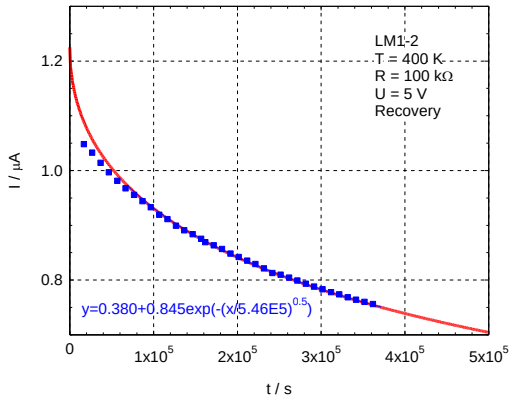

Fig. 8. DCL vs. time characteristic of sample LM1-2 at temperature 400 K, applied voltage U = 5 V.

DCL vs. time characteristic for DCL recovery can be fitted by equation:

$$I = I_0 + I_1\left(\exp\left(-\left(t/\tau\right)^n\right)\right) \tag{5}$$

where I_0 = 0.38 μA, I_1 = 0.845 μA, τ = 5.46x10^5 s and exponent n = 0.5 for sample LM1–2 at temperature 400 K and applied voltage U = 5 V (see Fig. 8). The time constant for the DCL value recovery is in this case of the order of 10^5 s for all the measured samples.

We have applied recovery process for the time interval 2x10^6 s (550 h), the results of this experiment shown in Fig. 9 for samples of ensemble LM 1, in Fig. 10 for samples of ensemble LN1, and in Fig. 11 for samples of ensemble LT8, respectively. In these Figures the first bar (red color) corresponds to the initial value of DCL before thermal treatment, the second bar (blue color) corresponds to value of DCL after the 20 days of ageing and the third bar (green color) corresponds to value of DCL after recovery for 550 h.

I average [μA]	Before ageing	After Ageing	After Recovery
Producer A	4.7	21.3	11.4
Producer B	5.7	24	5.1
Producer C	2.4	37.8	6

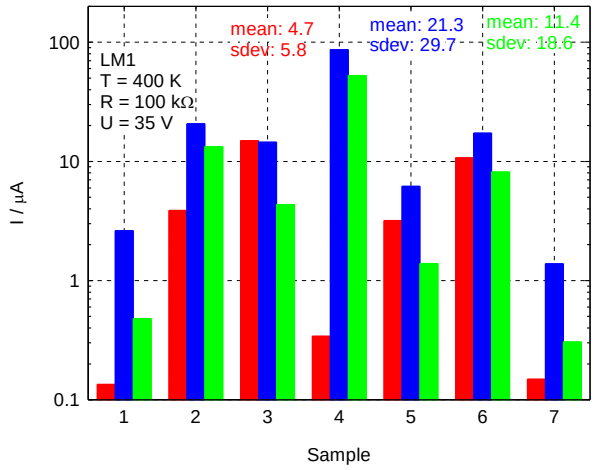

Fig. 9. Bar chart diagram of ensemble LM1 for DCL original value (red), DCL value after ageing (blue) and DCL after annealing (green)

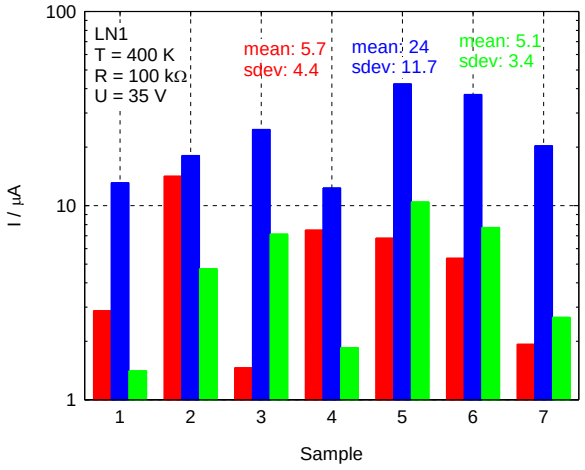

Fig. 10. Bar chart diagram of ensemble LN1 for DCL original value (red), DCL value after ageing (blue) and DCL after annealing (green)

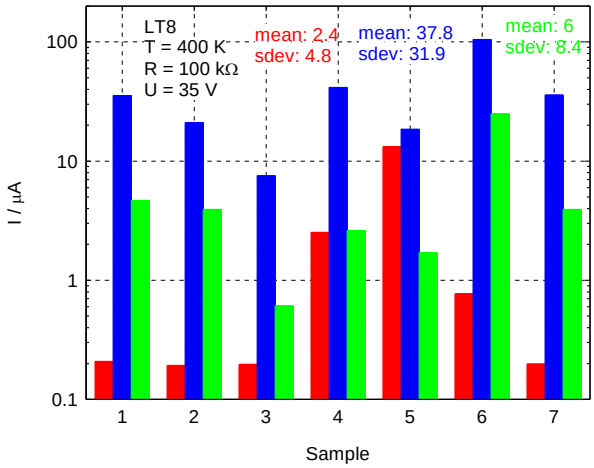

Fig. 11. Bar chart diagram of ensemble LT8 for DCL original value (red), DCL value after ageing (blue) and DCL after annealing (green)

I-V characteristics of some samples were improved during the thermal treatment and partial discharges disappeared. The observation of all samples proved that thermal annealing under the external electric field leads to the DCL increase, and its value can be recovered when the external electric field is eliminated.

CONCLUSION

1. The dominant current transport mechanism in normal mode at T = 300 K is Ohmic for electric field less than 1 MV/cm, and for higher value of electric field the tunneling electron transport is observed.
2. Experimental results at temperature T = 400 K show that DCL consists of 3 parallel current components; Ohmic, Poole-Frenkel and tunneling current components.
3. DCL for applied voltage U = 35 V in normal mode measured at fixed temperature 400 K increases exponentially with time with decreasing value of the first derivative dI(t)/dt. DCL value saturation was not observed even after the 20 days of thermal annealing. We suppose that the DCL increase is influenced by the ions redistribution in the tantalum pent-oxide layer. Positive ions (oxygen vacancies) drift in electric field close to the cathode interface, which influences/decreases the height of potential barrier formed on the Ta_2O_5 – MnO_2 interface.
4. Leakage current variations are reversible. Thermal annealing with eliminated external electric field resulted in a gradual decrease of leakage currents and restored their values very near to the initial ones.

ACKNOWLEDGEMENTS

Research described in the paper was financially supported by the European Centres of Excellence CEITEC CZ.1.05/1.1.00/02.0068 and by the project Sensor, Information and Communication Systems CZ.1.05/2.1.00/03.0072.

REFERENCES

[1] A. Teverovsky, Effect of Post-HALT Annealing on Leakage Currents in Solid Tantalum Capacitors, in Capacitor and Resistor Technology Symposium, CARTS USA 2010, p. 43-59, (2010)
[2] J. Sikula et al., Tantalum and Niobium Oxide High Voltage Capacitors: Field Crystallization and Leakage Current Kinetics, in Capacitor and Resistor Technology Symposium, CARTS EU 2008, p.267-276, (2008)
[3] J. Sikula et al., Ta and NbO High Voltage Capacitors: Leakage Current Kinetics for MnO2 and Conducting Polymer Cathode, in Capacitor and Resistor Technology Symposium, CARTS USA 2009, Jacksonville, FL, pp. 337-345, (200.
[4] T. Zednicek, J. Sikula, and H. Leibovitz, "A Study of Field Crystallization in Tantalum Capacitors and its effect on DCL and Reliability," in Capacitor and Resistor Technology Symposium, CARTS USA 2009, Jacksonville, FL, pp. 305-320, (2009).
[5] R. M. Fleming, et al., "Defect dominated charge transport in amorphous Ta2O5 thin films," Journal of Applied Physics, vol. 88, pp. 850-862, Jul 15 2000.
[6] J. Sikula et al, „Ion Diffusion and Field Crystallization in Niobium Oxide Capacitors“ in Capacitor and Resistor Technology Symposium, CARTS Europe, Nice, France, 2011, p. 3-33–41.
[7] A. Teverovsky, "Reverse bias behavior of surface mount tantalum capacitors," in Capacitor and Resistor Technology Symposium, CARTS, New Orleans, LA, 2002, pp. 105-123